ELSEVIER

Journal of Organometallic Chemistry 550 (1998) 89–99

Journal of Organometallic Chemistry

Vibrational spectroscopy and solid-state MAS NMR studies of mercury(II) acetate complexes [Hg(X)OAc] Crystal structure of [Hg(CN)OAc] [1]

Graham A. Bowmaker [2], Andrei V. Churakov [3], Robin K. Harris *, Se-Woung Oh [4]

Department of Chemistry, University of Durham, South Road, Durham DH1 3LE, UK

Received 3 January 1997

Abstract

The syntheses of [Hg(X)OAc] (OAc = acetate; X = CN, Cl, Br, I, SCN) are reported, and the crystal structure of the cyano complex has been determined. The asymmetric unit contains two [Hg(CN)OAc] molecules which show almost linear C–Hg–O bonding (Hg–C = 2.019(13), 2.016(11) Å; Hg–O = 2.067(9), 2.058(8) Å; C–Hg–O = 176.0(4), 172.3(5)°), with only one of the two acetate oxygen atoms bound directly to the mercury atom. Secondary Hg · · · O and Hg · · · N contacts in the range 2.6–2.8 Å are about 0.2 Å shorter than the secondary Hg · · · O contacts in the corresponding X = Ph complex. The ν(HgX) and ν(HgO) modes have been assigned in the IR and Raman spectra of [Hg(X)OAc] (X = CN, Cl, Br, I, SCN); these spectra show that the complexes have structures with essentially linear O–Hg–X bonding, similar to that of the cyanide. Solid-state ^{199}Hg MAS NMR spectra have been recorded for HgX_2 (X = CN, Cl) and [Hg(X)OAc] (X = Me, Ph, CN, Cl, SCN), and spinning sideband analysis has been used to determine the ^{199}Hg shielding anisotropy and asymmetry parameters $\Delta\sigma$ and η. A semi-empirical method for the calculation of the local paramagnetic contribution to the shielding is given, and a linear relationship between $\Delta\sigma$ and the isotropic shielding σ_{iso} which is predicted by this model for linear HgXY species is found to be obeyed reasonably well by the experimental data for HgX_2 and [Hg(X)OAc]. The same method is used to analyse the effects of secondary bonding on the ^{199}Hg shielding parameters. The ^{13}C MAS NMR spectrum of [Hg(SCN)OAc] shows $^2J(^{199}Hg^{13}C)$ and $^3J(^{199}Hg^{13}C)$ coupling to the acetate carbon atoms, with magnitudes similar to those found previously for $Hg(OAc)_2$. The CN carbon signals in $Hg(CN)_2$ and [Hg(CN)OAc] are split into 2:1 doublets due to residual dipolar coupling to the quadrupolar ^{14}N nucleus. © 1998 Elsevier Science S.A.

Keywords: MAS NMR; Hg(X)OAc; Crystal structure

1. Introduction

With the developments which have taken place in high-resolution NMR techniques for solids [1–10], there has been increasing interest in the solid-state NMR spectra of heavy metal nuclei [4,5]. Until recently, there were very few solid-state NMR studies involving ^{199}Hg, but in the last few years there has been a considerable increase in the number of such investigations [4,5,11–17]. The first compound for which a ^{199}Hg MAS NMR spectrum was reported was mercury(II) acetate, $Hg(OAc)_2$ [12], and this compound has subsequently been the subject of a number of further ^{199}Hg solid-state NMR studies [13,14,18,19]. Mercury(II) acetate has also been studied by ^{13}C CP MAS NMR spectroscopy [20]. This showed separate signals from the two acetate groups, in agreement with the crystal structure of the compound [21]. The spectrum also showed $^2J(^{199}Hg^{13}C)$ satellites on the carbonyl carbon signals, and $^3J(^{199}Hg^{13}C)$ satellites on the methyl carbon signals. This coupling is not evident in the solution-state spectrum, despite the narrower lines observed in solution,

* Corresponding author. Tel.: (+44) 191 374 3121; fax: (+44) 191 386 1127; e-mail: r.k.harris@durham.ac.uk

[1] Dedicated to Professor Ken Wade on the occasion of his 65th birthday in recognition of his outstanding contributions to inorganic and organometallic chemistry.

[2] Permanent address: Department of Chemistry, University of Auckland, Private Bag 92019, Auckland, New Zealand.

[3] Permanent address: N.S. Kurnakov Institute of General and Inorganic Chemistry, Russian Academy of Science, 31 Leninskii prospekt, Moscow 117907, Russia.

[4] Present address: Department of Chemistry, Mokpo National University, Muan, Chonnam 534-729, South Korea.

because of the occurrence of ligand-exchange processes. Consequently, it was suggested that solid-state ^{13}C NMR spectroscopy might be of value in characterising other organometallic compounds through the observation of long-range couplings which are not detectable in solution [20].

In the present work we have extended the above studies to the compounds [Hg(X)OAc] (X = Me, Ph, CN, Cl, Br, I, SCN). The only compound in this series whose crystal structure has been reported is [Hg(Ph)OAc], and this shows that the solid contains discrete molecules in which the mercury atom is bound covalently to the phenyl ring on one side and to one of the acetate-oxygen atoms on the other to give an almost linear C–Hg–O coordination environment [22]. The only report of a mixed halide–acetate complex of mercury(II) is [Hg(I)OAc], which is formed in the reaction between HgI_2 and $Hg(OAc)_2$ in glacial acetic acid [23]. The original report of this compound suggested that it is metastable in the solid state, decomposing back into $Hg(OAc)_2$ and red HgI_2 upon standing for a few hours [23].

A number of empirical correlations between anisotropic ^{199}Hg shielding parameters and structure have been discussed in the literature. Most of these have involved mercury(II) complexes with thiolate ligands, since it is for this class of complex that data for series of closely related compounds are available [11,14–17]. In order to extend these correlations, and to put them on a more quantitative basis, it was considered desirable to obtain similar data for other series of compounds with different types of ligand. The two main aims of the present study were to characterize a range of mixed-ligand complexes of the type [Hg(X)OAc], and to investigate the dependence of the ^{199}Hg shielding tensor parameters on the nature of X. Of the new compounds prepared, the only one for which it has proved feasible to determine the crystal structure is [Hg(CN)OAc]. The IR and Raman spectra of the X = Cl, Br, I, CN, SCN complexes were therefore studied in order to determine whether any major structural changes occur within this series. In view of the unusual observation of long-range couplings by other workers in the solid-state ^{13}C NMR spectrum of $Hg(OAc)_2$ [20], the ^{13}C MAS NMR spectra of [Hg(X)OAc] were also studied in this work. For comparison purposes, the ^{199}Hg MAS NMR spectra of $HgCl_2$ and $Hg(CN)_2$ and the ^{13}C MAS NMR spectrum of $Hg(CN)_2$ were also recorded.

2. Experimental

2.1. Materials

Commercial samples of mercury(II) cyanide $Hg(CN)_2$, mercury(II) thiocyanate $Hg(SCN)_2$, mercury(II) acetate, $Hg(OAc)_2$ (Aldrich), methyl mercury acetate [Hg(Me)OAc], phenyl mercury acetate [Hg(Ph)OAc] (Ventron), and mercury(II) chloride $HgCl_2$ (Hopkin and Williams) were used without further purification.

2.2. Synthesis of halogeno- and cyano-(acetato)-mercury(II), [Hg(X)OAc] (X = Cl, Br, I, CN)

The preparations of the X = Cl, Br, I, CN compounds are very similar, so that the preparation of the cyanide is given here as a representative case. To a solution of mercury(II) acetate, $Hg(OAc)_2$ (0.74 g, 2.31 mmol) in warm glacial acetic acid (15 cm^3) was added solid $Hg(CN)_2$ (0.58 g, 2.31 mmol). The $Hg(CN)_2$ dissolved completely upon heating the solution to near boiling. The colourless crystalline solid which was obtained upon cooling the solution was collected, washed with glacial acetic acid (4 cm^3), and air-dried. Yield 0.97 g (73%). M.p. 201–202 °C. Anal. Found: C, 12.6; H: 1.0; N, 4.8. Calc. for $C_3H_3HgNO_2$: C, 12.61; H, 1.06; N, 4.90%. Crystals for the X-ray structure determination were grown by very slow cooling of a glacial acetic acid solution produced by the preparative method described above. For the preparation of the X = Cl complex, less glacial acetic acid (9 cm^3) is required, due to the greater solubility of this compound. For the X = I complex, a 50% excess of $Hg(OAc)_2$ is required (see Section 3). Melting points and analytical data for the halogeno-complexes (all colourless solids) are as follows: [Hg(Cl)OAc], m.p. 145–149 °C. Anal. Found: C, 8.3; H: 0.9. Calc. for $C_2H_3ClHgO_2$: C, 8.14; H, 1.10%; [Hg(Br)OAc], m.p. 164–167 °C. Anal. Found: C, 7.1; H: 0.8. Calc. for $C_2H_3BrHgO_2$: C, 7.07; H, 0.89%; [Hg(I)OAc], m.p. 146–149 °C. Anal. Found: C, 6.5; H: 0.7. Calc. for $C_2H_3HgIO_2$: C, 6.21; H, 0.78%.

2.3. Synthesis of thiocyanato(acetato)mercury(II), [Hg(SCN)OAc]

The preparative method for this complex is similar to that described above for the cyanide, the main differences being due to the much lower solubility of $Hg(SCN)_2$ and [Hg(SCN)OAc] in glacial acetic acid: $Hg(SCN)_2$ (0.73 g, 2.31 mmol) was added to nearly boiling glacial acetic acid (200 cm^3), and the hot solution of $Hg(SCN)_2$ was decanted from the small amount of undissolved solid which remained. To this solution was added a solution of $Hg(OAc)_2$ (0.74 g, 2.31 mmol) in glacial acetic acid (15 cm^3). The colourless crystalline solid which was obtained upon cooling the solution was collected, washed with glacial acetic acid, and air-dried. Yield 1.05 g (72%). M.p. dec. > 200 °C. Anal. Found: C, 11.2; H: 0.8; N, 4.3. Calc. for $C_3H_3HgNO_2S$: C, 11.34; H, 0.95; N, 4.41%.

Table 1
Crystal data and structure refinement for $[Hg(CN)O_2CCH_3]$

Formula	$C_3H_3HgNO_2$
Formula weight	285.65
Crystal system	monoclinic
Space group	$P2_1/c$
a/Å	7.775(1)
b/Å	11.940(2)
c/Å	11.917(2)
β/deg	104.34(1)
Volume/Å^3	1071.8(3)
Z	8
Density (calculated)/g cm^{-3}	3.541
Absorption coefficient/mm^{-1}	28.6
$F(000)$	992
θ range for data collection/deg	2.4 to 27.5
Index ranges	$10 \geq h \geq -8$, $15 \geq k \geq -13$, $14 \geq l \geq -15$
Reflections collected	7642
Independent reflections	2443 [R(int) = 0.109][a]
Observed reflections, $I > 2\sigma(I)$	2265
Data/parameters	2443/131
Goodness of fit on F^2	1.119
Final R indices [$I > 2\sigma(I)$]	$R1 = 0.0580$ $wR2 = 0.1545$
Final R indices (all data)	$R1 = 0.0609$ $wR2 = 0.1591$
Largest diff peak and hole/e Å^{-3}	3.36, −1.92

[a] Before absorption correction, R(int) = 0.174.

2.4. X-ray crystallography

Single crystals of $Hg(CN)(CH_3CO_2)$ were obtained by slow cooling of a glacial acetic acid solution, as described above. A colourless crystal of dimensions $0.40 \times 0.25 \times 0.20$ mm^3 was mounted on the tip of a glass fibre using perfluorinated oil. Preliminary examination and data collection were performed at 150.0(2) K on a three-circle Siemens SMART diffractometer with CCD area detector, using graphite-monochromatized Mo Kα radiation ($\lambda = 0.71073$ Å). Cell parameters were determined from 73 centred reflections and refined during data processing using all diffraction data (Siemens SAINT program) [24]. An empirical absorption correction based on measurements of equivalent reflections was applied (SHELXTL/VMS [25], $T_{min,max} = 0.001, 0.018$).

The structure was solved by direct methods (SHELXS-86) [26] and refined by full-matrix least squares on F^2 of all reflections (SHELXL-93) [27] with anisotropic thermal parameters for all non-hydrogen atoms. Methyl groups were refined using a rigid-body model (d(C-H) = 0.98 Å) with refined U_{iso}. The weighting scheme $w^{-1} = [\sigma^2(F^2) + a(P^2) + b(P)]$ was used, where $3P = (2F_c^2 + F_o^2)$, $a = 0.1013$ and $b = 7.1771$.

SHELXTL [25] software was used to prepare material for publication. Data reduction was performed using a DEC Alpha Station, whereas structure solution and refinement were made with a Silicon Graphics Irix Indigo Workstation.

Table 2
Atomic fractional coordinates ($\times 10^4$) and equivalent isotropic displacement parameters (Å$^2 \times 10^3$) for $[Hg(CN)O_2CCH_3]$

Atom	x	y	z	U_{eq} [a]
Hg(1)	6707.9(6)	5448(4)	6797.3(4)	32.9(2)
C(1)	5273(16)	6912(11)	4971(11)	33(2)
C(2)	5155(20)	7903(14)	4185(13)	47(3)
O(1)	6820(12)	6789(7)	5719(9)	37(2)
O(2)	4037(12)	6227(8)	4891(8)	36(2)
C(5)	6586(16)	4219(11)	7938(10)	35(2)
N(1)	6566(18)	3515(12)	8586(11)	51(3)
Hg(2)	1133.7(6)	6735.0(4)	5410.2(4)	32.9(2)
C(3)	1182(17)	5056(10)	7048(10)	34(2)
C(4)	1731(19)	4398(12)	8133(11)	40(3)
O(3)	2270(12)	5801(8)	6856(8)	38(2)
O(4)	−317(11)	4924(8)	6326(8)	37(2)
C(6)	−121(16)	7776(11)	4137(11)	36(3)
N(2)	−802(18)	8313(11)	3351(12)	48(3)

[a] The equivalent isotropic displacement parameter U_{eq} is defined as one-third of the trace of the orthogonalized $\mathbf{U}_{ij}$ tensor.

Crystal data as well as data collection and refinement parameters are given in Table 1. Final atomic coordinates, and selected bond lengths and angles are listed in Tables 2 and 3 respectively. The molecular structure, and the arrangement of the molecules in the crystal lattice of [Hg(CN)OAc] are shown in Figs. 1 and 2 respectively. Further details are available from the Director of the Cambridge Crystallographic Data Centre, 12 Union Road, Cambridge CB2 1EZ, UK.

Table 3
Selected intramolecular and intermolecular distances and angles for $[Hg(CN)O_2CCH_3]$

Distances/Å			
Hg(1)–C(5)	2.019(13)	Hg(2)–C(6)	2.016(12)
Hg(1)–O(1)	2.067(9)	Hg(2)–O(3)	2.058(8)
Hg(1)–O(4A)	2.589(9)	Hg(2)–O(3)	2.557(9)
Hg(1)–N(2B)	2.754(12)	Hg(2)–N(1D)	2.844(14)
Hg(1)–O(2A)	2.795(9)	Hg(2)–O(4)	2.784(10)
Hg(1)–O(2)	2.829(9)	Hg(2)–O(4C)	2.820(9)
C(1)–O(1)	1.32(2)	C(3)–O(3)	1.29(2)
C(1)–O(2)	1.25(2)	C(3)–O(4)	1.28(2)
C(1)–C(2)	1.50(2)	C(3)–C(4)	1.48(2)
C(5)–N(1)	1.14(2)	C(6)–N(2)	1.15(2)
Angles/deg			
C(5)–Hg(1)–O(1)	176.0(4)	C(6)–Hg(2)–O(3)	172.3(5)
O(1)–Hg(1)–O(4A)	82.8(3)	O(3)–Hg(2)–O(2)	81.5(3)
O(4A)–Hg(1)–N(2B)	76.0(4)	O(3)–Hg(2)–N(1D)	87.6(4)
O(1)–Hg(1)–O(2A)	98.0(3)	O(3)–Hg(2)–O(4C)	101.9(3)
O(1)–Hg(1)–O(2)	51.8(3)	O(3)–Hg(2)–O(4)	51.9(3)
O(2)–C(1)–O(1)	122.5(12)	O(4)–C(3)–O(3)	119.8(11)
O(2)–C(1)–C(2)	122.9(12)	O(4)–C(3)–C(4)	122.7(12)
O(1)–C(1)–C(2)	114.6(11)	O(3)–C(3)–C(4)	117.5(11)
C(1)–O(1)–Hg(1)	109.6(8)	C(3)–O(3)–Hg(2)	111.0(8)
N(1)–C(5)–Hg(1)	178.0(12)	N(2)–C(6)–Hg(2)	174.7(13)

Symmetry transformations used to generate equivalent atoms: O(4A) $1+x, y, z$; N(2B), $1+x, 1.5-y, 0.5+z$; O(2A), $1-x, 1-y, 1-z$; O(4C), $-x, 1-y, 1-z$; N(1D), $1-x, 0.5+y, 1.5-z$.

2.5. MAS NMR spectroscopy

^{13}C and ^{199}Hg MAS spectra were obtained, at 75.43 MHz and 53.62 MHz respectively, using a Varian Unity Plus 300 spectrometer. A 5.0 mm o.d. silicon nitride rotor with Vespel end-caps was used for all spectra, with spin rates in the range 6–13 kHz. Although measurements were nominally made at ambient probe temperature (ca. 25 °C), it is likely that the fast spinning used for the ^{199}Hg spectra resulted in substantially elevated temperatures (ca. 45 °C) [28]. For both nuclei, high-power proton decoupling (equivalent to 60 kHz) was used where appropriate. Cross-polarization (with flip-back) was employed for the ^{13}C spectra of all compounds except $Hg(CN)_2$ and [Hg(CN)OAc], for which direct polarization was used. Optimum contact times for [Hg(X)OAc] were estimated to be 8 ms (X = Cl, Br, I) and 20 ms (X = SCN). For the ^{13}C spectra, recycle delays of 30 s (X = Cl, Br, I) and 5 s (X = CN, SCN) were used. The number of transients required for good-quality spectra was between 100 and 1000 (with cross-polarization) and about 20 000 (with direct polarization). ^{199}Hg spectra were recorded with direct polarization (1 μs 12° pulses as judged via cross-polarization for a sample of $[Hg(dmso)_6][O_3SCF_3]_2$). Centreband signals were located by varying the spinning rate. Recycle delays of 3 s with ca. 20 000 transients were required to get acceptable spectra. Spinning sideband intensities were analysed to yield values of the shielding tensor components by an iterative computer program written in-house [29]. The fitting procedure used a minimum of ten sidebands plus the centreband, and was carried out for spinning rates in the range 6630–13 200 Hz. Accuracy was limited by the high noise levels, and because the spectra required baseline correction. Errors in the shielding tensor parameters were calculated by a published method [30]. They are statistical in nature, and may underestimate the true errors, which would also have systematic and experimental reproducibility contributions. Chemical shifts were referenced using replacement samples of adamantane ($\delta_C = 38.4$ ppm for the CH_2 carbon on the tetramethylsilane scale) and $[Hg(dmso)_6][O_3SCF_3]_2$ ($\delta_{Hg} = -2313$ ppm [31] on the dimethylmercury scale).

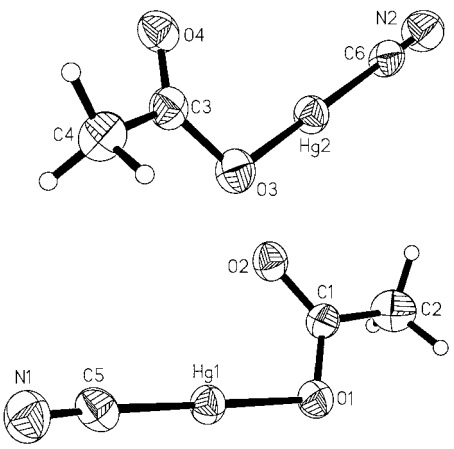

Fig. 1. Molecular structure of $[Hg(CN)(CH_3CO_2)]$. Displacement ellipsoids are shown at 50% probability level.

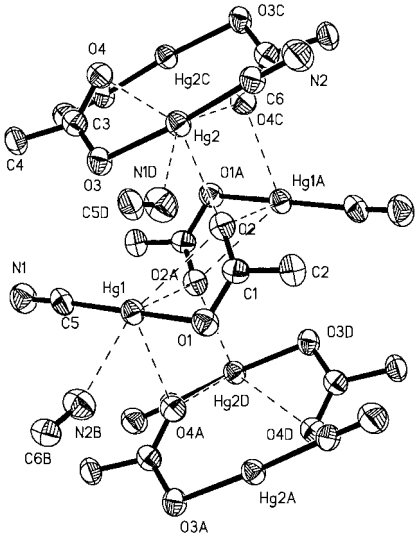

Fig. 2. Part of the crystal lattice of $[Hg(CN)(CH_3CO_2)]$, showing the secondary interactions.

2.6. Vibrational spectroscopy

Infrared spectra were recorded with 4 cm^{-1} resolution at room temperature as KBr discs on a Digilab FTS-60 Fourier-transform infrared spectrometer employing an uncooled DTGS detector. Far-infrared spectra were recorded with 2 cm^{-1} resolution at room temperature as pressed polythene discs on a Digilab FTS-60 Fourier-transform infrared spectrometer employing an FTS-60V vacuum optical bench with a 6.25 μm mylar film beam splitter, a mercury lamp source and a pyroelectric triglycine sulphate detector. Raman spectra were recorded at 4.5 cm^{-1} resolution using a Jobin–Yvon U1000 spectrometer equipped with a cooled photomultiplier (RCA C31034A) detector. The 488.0 nm exciting line from a Spectra-Physics Model 2016 argon-ion laser was used.

3. Results and discussion

3.1. Syntheses

The complexes [Hg(X)OAc] (X = CN, Cl, Br, I, SCN) were readily prepared in general by mixing equimolar amounts of HgX_2 and $Hg(OAc)_2$ in hot

glacial acetic acid. In the case of the X = I compound, it was found necessary to use a 50% excess of $Hg(OAc)_2$. If the excess $Hg(OAc)_2$ was not present, the product was found to be contaminated with yellow HgI_2, which gradually reverted to red HgI_2 on standing. This is probably the reason for the original observation that the product of the 1:1 reaction is a yellow solid which turns red upon standing for a few hours [23]. However, the present study shows that [Hg(I)OAc], like the other members of the series, is a colourless solid which is stable under ambient conditions.

3.2. Crystal structure of [Hg(CN)OAc]

The molecular structure and the arrangement of the molecules in solid [Hg(CN)OAc] are shown in Figs. 1 and 2. Selected distances and angles are given in Table 3. The asymmetric unit contains two [Hg(CN)OAc] molecules with closely similar structures. These have almost linear C–Hg–O bonding, with only one of the two acetate oxygen atoms bound directly to the mercury atom. The cyanide ligands are almost collinear with the Hg–C bond direction. In the structural chemistry of mercury(II), it is frequently found that there are weaker secondary interactions as well as the primary bonding interactions involving the 'characteristic' linear twofold-coordination of mercury [32–37]. In the present case there are two O atoms (which are bonded to Hg of another molecule) and one N atom which lie in a plane approximately perpendicular to the primary C–Hg–O bonding direction, at distances in the range 2.6–2.8 Å (Fig. 2, Table 3). Comparing these with the appropriate van der Waals radii sums, Hg,O = 3.04, Hg,N = 3.10 Å [38,39], it is apparent that these contacts represent secondary bonding interactions. The only other atom which is at a distance less than 3.1 Å from the mercury atom is the non-bonded oxygen atom of the same acetate ligand, at a distance of about 2.8 Å (see discussion below). The mercury atom environment is similar to that in [Hg(Ph)OAc], but in the latter case the non-bonded (or secondary bonding) contacts are about 0.2 Å longer [22]. A possible rationalization of this result is that the Ph^- ligand, being a stronger σ-donor than CN^-, places more electron density on the mercury atom, thus making it a poorer acceptor for secondary bonding interactions.

3.3. Vibrational spectra

The far-IR and low-wavenumber Raman spectra of [Hg(X)OAc] (X = CN, Cl, Br) are shown in Figs. 3 and 4. The wavenumbers and assignments of the bands in these spectra, and in those of the X = I, SCN complexes are given in Table 4. The bands in this region can be assigned to vibrations of the O–Hg–X units in these compounds. The bond-stretching modes of these units give rise to two bands (sometimes with a partially resolved splitting due to site-inequivalence or factor-group effects) which are essentially coincident in the IR and Raman spectra. One of these bands is strongly X-sensitive; its position in the IR spectra changes from 427 (X = CN) to 188 cm^{-1} (X = I), and this is assigned as ν(HgX). The other, at about 300 cm^{-1}, is much less dependent on X, and is assigned as ν(HgO). These descriptions are approximate, as some mixing of the Hg–X and Hg–O coordinates is expected in these modes. The consequences of this become evident in the spectra of the heavier X = Br, I, SCN members of the series, where the two bands show near mutual exclusion between the IR and Raman spectra (see Fig. 3(c) and Fig. 4(c) for the X = Br case), suggesting that the lower and higher wavenumber modes are similar in character to the symmetric and antisymmetric stretching modes of a linear HgX_2 species. The wavenumbers of the ν(HgX) modes decrease with increasing mass of X, and are similar to the average of the wavenumbers of the symmetric and antisymmetric modes of the corresponding

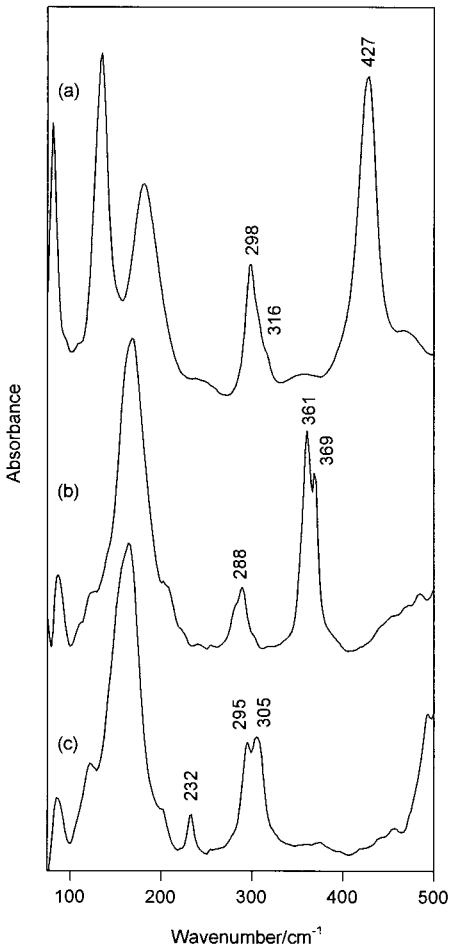

Fig. 3. Far-IR spectra of [Hg(X)OAc]: (a) X = CN, (b) X = Cl, (c) X = Br; bands assigned to ν(HgX) and ν(HgO) are labelled with their wavenumbers.

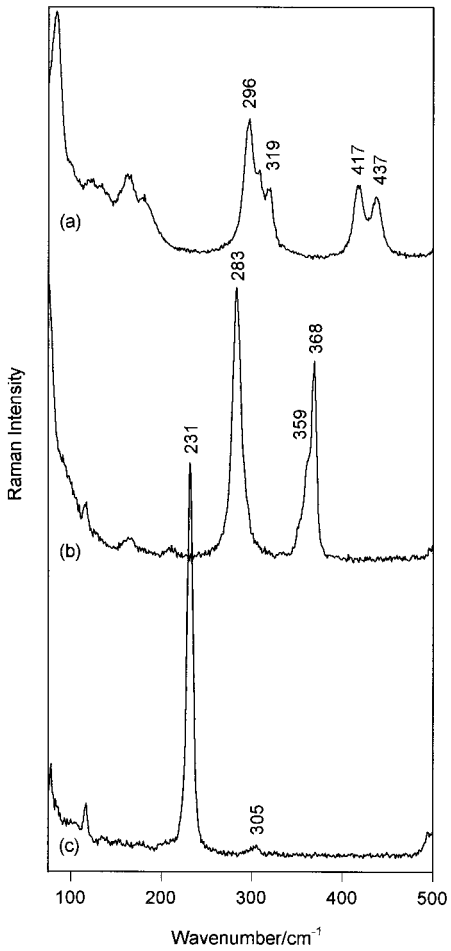

Fig. 4. Low-wavenumber Raman spectra (details as for Fig. 3).

HgX_2 solids [40,41]. The only other strong feature in the low-wavenumber spectra is a single band (X = Cl, Br, I) or a pair of bands (X = CN, SCN) in the 140–180 cm^{-1} region of the IR spectra. In the former compounds, these have been assigned as δ(OHgX) modes, as they show a decrease in frequency from X = Cl to X = I, and the activities (very strong in the IR; very weak or absent in the Raman spectra) correspond closely to those for the doubly degenerate bending mode of a linear HgX_2 species. The reason for the appearance of two bands in this region for the X = CN, SCN complexes is not known at present. We tentatively assign the higher wavenumber component to δ(OHgX); the lower wavenumber component may be due to a splitting of the δ(OHgX) mode (which would be doubly degenerate for a perfectly linear complex) or to some other unidentified mode.

The above observations lend strong support to the view that all of these compounds have similar structures, involving discrete [Hg(X)OAc] molecules with essentially linear O–Hg–X bonding. The mid-IR spectra all show bands due to coordinated acetate at wavenumbers similar to those in $Hg(OAc)_2$. In addition, the IR spectrum of [Hg(CN)OAc] shows ν(CN) = 2197, 2190 cm^{-1}, while that of [Hg(SCN)OAc] shows ν(CN) = 2139; δ(SCN) = 458, 428, 423 cm^{-1}.

3.4. ^{199}Hg MAS NMR spectra

The solid-state ^{199}Hg MAS NMR spectra of $Hg(CN)_2$ and [Hg(CN)OAc] are shown in Fig. 5. As with other mercury complexes which show large ^{199}Hg shielding anisotropy, the spectra consist of a centreband flanked by a number of spinning sidebands [4,5,11–17]. The chemical shift and shielding parameters obtained from a spinning sideband analysis of these spectra, and of the spectra of the other compounds studied in this work, are compared with those of some related compounds in Table 5. The principal components σ_{11}, σ_{22}, σ_{33} of the shielding tensor are defined such that

$$|\sigma_{33} - \sigma_{iso}| \geq |\sigma_{11} - \sigma_{iso}| \geq |\sigma_{22} - \sigma_{iso}| \quad (1)$$

where δ_{iso} is the isotropic, or scalar, shielding constant (relative to that of the reference), measured as

$$\sigma_{iso} = -\delta_{iso} \quad (2)$$

where σ_{iso} is the isotropic chemical shift (the centreband shift). Thus σ_{iso} is related to the principal components of the shielding tensor by

$$\sigma_{iso} = (1/3)(\sigma_{11} + \sigma_{22} + \sigma_{33}) \quad (3)$$

The shielding anisotropy is defined as

$$\Delta\sigma = \sigma_{33} - \tfrac{1}{2}(\sigma_{11} + \sigma_{22}) \quad (4)$$

Table 4
Low-wavenumber vibrational spectra (100–500 cm^{-1}) of [Hg(X)OAc]

Compound	IR/cm^{-1}	Raman/cm^{-1}	Assignment
[Hg(Cl)OAc]	369, 361	368, 359	ν(HgCl)
	288	283	ν(HgO)
	167	165	δ(OHgCl)
[Hg(Br)OAc]	305, 295	305	ν(HgO)
	232	231	ν(HgBr)
	164		δ(OHgBr)
[Hg(I)OAc]	297, 278	295, 278	ν(HgO)
	188	183	ν(HgI)
	157		δ(OHgI)
[Hg(CN)OAc]	427	437, 417	ν(HgC)
	316, 298	319, 296	ν(HgO)
	180	182, 163	δ(OHgC)
	134	134, 122	
[Hg(SCN)OAc]	318		ν(HgO)
	280	274	ν(HgS)
	165, 138	164, 142	δ(OHgS)
	103		

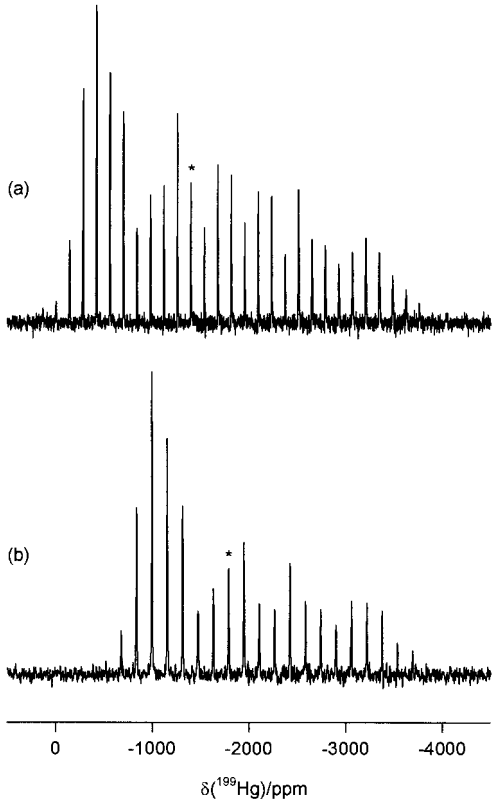

Fig. 5. 53.6 MHz ^{199}Hg MAS NMR spectra of (a) $Hg(CN)_2$ (spinning rate $\nu_s = 7500$ Hz), (b) [Hg(CN)OAc] ($\nu_s = 8560$ Hz). Baseline corrections and line-broadening (333 Hz) have been applied prior to plotting. The centreband is indicated by the asterisk.

and the departure of the shielding tensor from axial symmetry is described by the asymmetry parameter

$$\eta = (\sigma_{22} - \sigma_{11})/(\sigma_{33} - \sigma_{iso}) \quad (5)$$

^{199}Hg shielding tensor data have previously been determined for $HgCl_2$ and $Hg(CN)_2$ from measurements on static (non-rotating) samples, which permitted determination of the 'perpendicular' components σ_{11} and σ_{22} only; σ_{33} was calculated from σ_{iso} by using Eq. (3); σ_{iso} was assumed to be the same as the solution-state value [45]. In order to eliminate the uncertainties caused by the lower accuracy of static sample measurements and the assumption involved in the derivation of σ_{33} from the solution σ_{iso} value, we have measured the MAS NMR spectra of these compounds. The results are compared with those of the static measurements in Table 5.

Despite the fact that the crystal structure of [Hg(CN)OAc] shows the presence of two crystallographically inequivalent Hg atoms, there is only one signal and associated sideband pattern in the ^{199}Hg NMR spectrum. Thus, the isotropic shifts for the two sites are equal within the accuracy of the measurement ($\Delta\nu_{1/2} \approx 530$ Hz = 10 ppm), and the anisotropic parameters are the average of those for the two inequivalent molecules. In the case of [Hg(Cl)OAc], however, there are two clearly resolved ^{199}Hg signals, and separate sets of parameters have been derived for each. [Hg(Br)OAc] showed only a very weak signal at a position similar to

Table 5
^{199}Hg chemical shift and shielding tensor parameters (from ^{199}Hg MAS NMR spectra unless otherwise indicated)

Compound	σ_{11}/ppm	σ_{22}/ppm	σ_{33}/ppm	δ_{iso}/ppm	$\Delta\sigma$/ppm	η	Ref.
$HgMe_2$ [a]	−2450	−2450	4890	0	7325(55)	0	[42,43]
$HgPh_2$	−1122	−699	4307	−829	5218	0.12	[13]
$Hg(CN)_2$ [b]	−30	−30	3770	−1240	3800	0	[44]
$Hg(CN)_2$ [c]	193(5)	223(5)	3310(480)	−1240(150)[d]	3100(480)[e]	~0	[45]
$Hg(CN)_2$	33(34)	381(31)	3773(39)	−1396	3566(58)	0.15(2)	—[f]
$HgCl_2$ [c]	410(15)	410(15)	3800(170)	−1540(170)[d]	3390(170)[e]	0	[45]
$HgCl_2$	282(27)	573(26)	4019(26)	−1625	3592(37)	0.12(2)	—[f]
$Hg(SCN)_2$	81(23)	428(21)	3390(24)	−1300	3135(37)	0.17(2)	[46]
$Hg(OAc)_2$	1859	1947	3685	−2497	1782	0.07	[19]
Hg(Ph)OAc	187	375	3935	−1499	3654	0.08	[13]
	47(38)	534(32)	3919(44)	−1500	3629(66)	0.20(2)	—[f]
Hg(Me)OAc	−433(58)	−34(52)	3948(64)	−1160	4182(96)	0.14(3)	—[f]
Hg(Cl)OAc[g]	827(80)	888(80)	3837(22)	−1850	2981(33)	0.03(8)	—[f]
	880(84)	1051(84)	3795(23)	−1909	2831(34)	0.09(9)	
Hg(SCN)OAc	770(19)	1035(17)	3481(17)	−1762	2579(26)	0.15(2)	—[f]
Hg(CN)OAc	800(28)	830(28)	3724(10)	−1785	2909(15)	0.02(3)	—[f]

[a] From liquid crystal spectra.
[b] From solution-state relaxation time measurements.
[c] Static (non-rotating) sample.
[d] Average values from solution-state spectra.
[e] Calculated by using the isotropic shielding parameter from solution spectra.
[f] This work.
[g] Multiple signals due to site inequivalence.

that of the chloride, but the S/N ratio was insufficient to allow a spinning sideband analysis to be carried out. [Hg(I)OAc] yielded no detectable ^{199}Hg signal. The ^{199}Hg CP MAS NMR spectrum of [Hg(Ph)OAc] has been reported previously at a magnetic field strength of 2.35 T [13]. The results of the present higher-field measurement are in good agreement with the previously published ones, and the observation of a single signal is consistent with the crystal structure [22]. The spectrum of [Hg(Me)OAc], recorded for the first time in this work, shows only a single ^{199}Hg NMR signal.

We have recently shown that anisotropic ^{199}Hg shielding parameters can be interpreted on the basis of the expressions which have been derived for the local paramagnetic contribution to the shielding [46]. Within the (admittedly rather severe) inaverage excitation energy (AEE) approximation, the expressions for the principal components of the local paramagnetic shielding tensor for the case where the shielding is due to electron density in the valence p orbitals only, and the local symmetry is sufficiently high that cross terms in the charge-density matrix are zero, are:

$$\sigma_{xx} = (n_y + n_z - n_y n_z)\,\sigma_p \quad (6)$$

$$\sigma_{yy} = (n_x + n_z - n_x n_z)\,\sigma_p \quad (7)$$

$$\sigma_{zz} = (n_x + n_y - n_x n_y)\,\sigma_p \quad (8)$$

where n_x, n_y, n_z are the populations of the Hg $6p_x$, $6p_y$, $6p_z$ orbitals respectively, and

$$\sigma_p = -\mu_0 e^2 \hbar^2 \langle r^{-3} \rangle_{np} / 4\pi m^2 \Delta E \quad (9)$$

where μ_0 is the permeability constant, e is the elementary charge, m is the electron rest mass, ΔE is the average excitation energy, and $\langle r^{-3} \rangle_{np}$ is the expectation value of r^{-3} for the valence np electrons [47,48]. The average, or isotropic, local paramagnetic shielding derived from the above is

$$\sigma_{iso} = (1/3)(2n_x + 2n_y + 2n_z - n_x n_y - n_y n_z - n_x n_z)\,\sigma_p \quad (10)$$

For linear two-coordinate compounds HgX_2 involving the σ-donor (non-π-donor) ligand X, the bonding involves electron donation from the σ-donor orbital of X (or X^- if HgX_2 is a neutral complex) into the Hg $6p_z$ orbital (the z axis lies along the Hg–X bond direction), and the only non-zero orbital population in Eqs. (6)–(8) is the $6p_z$ population n. This yields $\sigma_{xx} = \sigma_{yy} = n\sigma_p$; $\sigma_{zz} = 0$. Since σ_p is negative (Eq. (9)), this yields $\sigma_{zz} > \sigma_{xx} = \sigma_{yy}$. If it is assumed that the diamagnetic contributions to the shielding are isotropic, and so contribute equally to all three principal components of the shielding tensor, the above relationship should also hold for the total shielding constants. Defining the principal axes of the shielding tensor according to Eq. (1) yields the relationship $\sigma_{33} > \sigma_{11} = \sigma_{22}$. Inspection of the results for HgX_2 (X = Me, Ph, Cl, CN, OAc) in Table 5 shows that the experimental values correspond closely to this relationship; the small deviations from equality of σ_{11} and σ_{22} in the solid-state data are due to small deviations from axial symmetry in the primary and/or secondary bonding interactions. Substitution of the above expressions for the shielding tensor components for linear HgX_2 into Eq. (4) yields $\Delta\sigma = -n\sigma_p$. Since σ_p is negative (Eq. (9)), $\Delta\sigma$ is positive. Thus $\Delta\sigma$ is proportional to the $6p_z$ population n which, in turn, is proportional to the σ-donor strength of the ligand, and so a strong σ-donor ligand, such as CH_3^-, will result in a greater n than will a weaker σ-donor, such as Cl^-. Therefore $\Delta\sigma$ is predicted to be greater for $HgMe_2$ than for $HgCl_2$, and the results in Table 5 show that this prediction is confirmed.

The above discussion applies essentially unchanged to linear mixed-ligand complexes HgXY. The only difference is that the Hg $6p_z$ orbital population consists of contributions from both the X and Y ligands, so that $\Delta\sigma$ for HgXY should be intermediate between the values for HgX_2 and HgY_2. Comparison of the results for [Hg(X)OAc] with those for HgX_2 (X = CH_3, Ph, Cl, CN, OAc) in Table 5 shows that this relationship is observed experimentally. In fact the $\Delta\sigma$ values for [Hg(X)OAc] are close to the arithmetic mean of the values for HgX_2 and $Hg(OAc)_2$, as shown in Fig. 6, and the above analysis gives a physical basis for this otherwise empirical observation.

In several cases of linear HgX_2 coordination involving secondary bonding, the asymmetry parameter remains close to zero due to the fact that the ligands

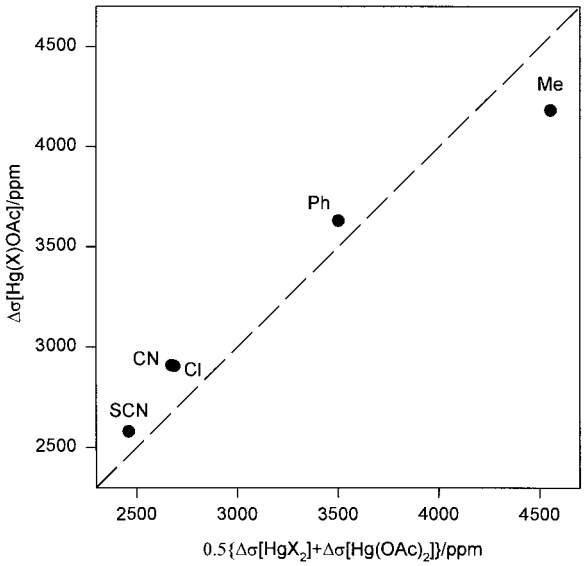

Fig. 6. Comparison of the observed shielding anisotropy $\Delta\sigma$ for [Hg(X)OAc] with the arithmetic mean of the anisotropies for HgX_2 and $Hg(OAc)_2$.

involved in the secondary bonding are symmetrically disposed about the X–Hg–X axis. This is illustrated by the case of $Hg(SCN)_2$, in which the primary S–Hg–S coordination is expanded to a distorted octahedral environment by the presence of weak interactions between the mercury atom and four N atoms of thiocyanate groups on neighbouring molecules [46]. This situation can be modelled by a linear HgX_2 unit along the z axis with secondary bonding to four ligands Y symmetrically placed along the x and y axes. The only modification required to the above treatment is that the $6p_x$ and $6p_y$ orbitals each have populations rn, where r is a fraction $(0 < r < 1)$ which is zero in the absence of secondary bonding. This yields

$$\Delta\sigma = -n(1-r)(1-rn)\sigma_p \qquad (11)$$

which shows that the effect of the secondary bonding $(r > 0)$ is to reduce $\Delta\sigma$. There is evidence that such a reduction occurs, and this will be discussed further below, in connection with the relationship between $\Delta\sigma$ and the isotropic shielding constant σ_{iso}.

The values of the asymmetry parameter η obtained for [Hg(X)OAc] (Table 5) are all less than 0.2 (small values of η are difficult to determine accurately [6,49]), implying that the shielding tensor is almost axially symmetric in these compounds. This is as expected for a linear HgXY complex (if the effect of the AC group is neglected). However, since the arrangement of atoms involved in the secondary bonding in [Hg(CN)OAc] is also not axially symmetric (see above), some deviation from $\eta = 0$ is expected, and it is perhaps surprising that this is so small. There are only three atoms in positions which are suitable for involvement in secondary bonding using the Hg $6p_x$, $6p_y$ orbitals (atoms O(2) and O(4) are not in positions suitable for overlap with these orbitals), and their arrangement can be described as follows. In a plane which is approximately perpendicular to the primary O–Hg–C bonds (z direction) there is one short Hg···O contact (2.6 Å; y direction), and two approximately perpendicular, longer contacts, Hg···O and Hg···N (2.8 Å; x direction). An η value of zero would result if the charge transfer into the Hg $6p_y$ orbital by the one strong secondary bond were equal to that transferred into the $6p_x$ orbital by the two weaker secondary bonds. Thus, the low asymmetry parameter η is consistent with the presence of secondary bonding, despite the non-axially symmetric arrangement of the atoms involved.

The isotropic shielding constants are obtained from the centreband shifts δ_{iso} (Eq. (2)), values of which are listed in Table 5 for the compounds studied in the present work. The relationship of this parameter to the electronic structure of the complex is given by Eq. (10). For the linear HgX_2 and HgXY cases this yields $\sigma_{iso} = (2/3)n\sigma_p$, compared with the corresponding expression derived above for the shielding anisotropy $\Delta\sigma = -n\sigma_p$, so that a plot of $\Delta\sigma$ vs. σ_{iso} should be linear, with a slope of -1.5. Such a plot for the various HgX_2 and [Hg(X)OAc] compounds in Table 5 is shown in Fig. 7. A linear relationship is indeed observed, but the slope is -2.2. One possible reason for this more negative slope is the presence of secondary bonding. It was shown above that such interactions lead to a reduction in $\Delta\sigma$ (Eq. (11)), and a similar analysis using Eq. (10) shows that σ_{iso} should decrease as well. This would result in the displacement of points towards lower $\Delta\sigma$ and σ_{iso}. Since the degree of secondary bonding increases with decreasing σ-donor strength of the ligands X,Y involved in the primary X–Hg–Y bonding (see above), this effect would result in a more negative slope for the line in Fig. 7. However, it seems likely that differences in the details of the secondary bonding would lead to deviations from the linear relationship, and this may be the reason for systematic deviations which appear to occur for the X = SCN compounds and, to a lesser extent, for the X = CN compounds. For this reason, the best fit line in Fig. 7 was determined without including the data for these compounds, although the result is not very different if these data are included.

Another possible reason for the increased negative slope of the line in Fig. 7 is that there are contributions to σ_{iso} from terms other than the local paramagnetic ones. Thus, terms such as those arising from the Fermi contact interaction, which are determined by electron density in the Hg 6s orbital, contribute equally to the anisotropic shielding parameters σ_{xx}, σ_{yy}, σ_{zz}, and so do not contribute at all to $\Delta\sigma$. The contribution of such terms to σ_{iso} should be proportional to the Hg 6s orbital

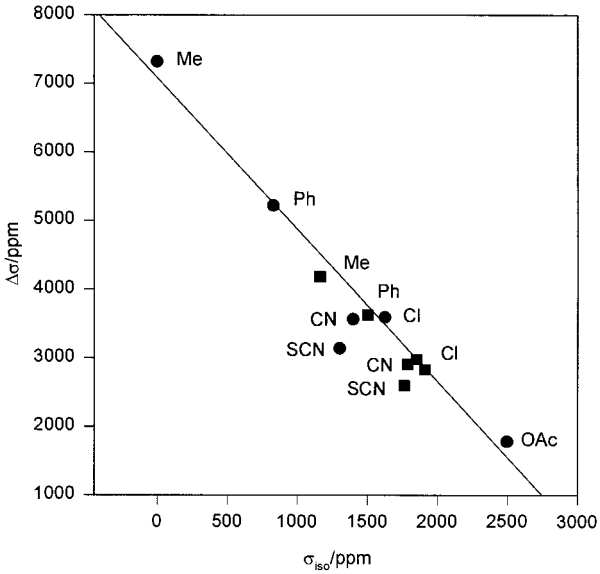

Fig. 7. Plot of the shielding anisotropy $\Delta\sigma$ for HgX_2 (●) and [Hg(X)OAc] (■) against the corresponding isotropic shielding constant σ_{iso}.

population, which is expected to increase with the Hg 6p population. Thus, the additional shielding arising from such terms will be greater for $HgMe_2$ than for $HgCl_2$, for example, implying that the data in Fig. 7 are displaced to the right by this effect, and that the extent of this displacement decreases with increasing σ_{iso}. This would also explain the increase in the negative slope of this graph relative to that predicted by the model involving local paramagnetic terms only.

It is not possible at this stage to determine which of the above effects is more important in accounting for the observed deviation in the slope from the predicted value, or whether there is some other explanation, such as a breakdown of the average excitation energy approximation, or a variation in the average excitation energy from one complex to another. This can probably only be determined by theoretical calculations of the shielding parameters. However, the fact that the relationship in Fig. 7 corresponds reasonably well to the predictions based on consideration of local paramagnetic effects alone supports the view that such effects play a dominant role in the isotropic and anisotropic shielding.

3.5. ^{13}C MAS NMR spectra

The ^{13}C MAS NMR parameters for [Hg(X)OAc] are given in Table 6. The spectra showed the expected signals due to the acetate ligand, but the long-range (^2J, ^3J) couplings to ^{199}Hg, which were observed in $Hg(OAc)_2$ [20], were only seen for the X = SCN complex. The X = Cl, Br, I compounds all showed doublet carbonyl carbon signals, indicating that there are two molecules in the asymmetric unit. This is consistent with the observation of two signals in the ^{199}Hg spectrum of the X = Cl complex; the observation of good quality ^{13}C spectra for the X = Br, I complexes, and the fact that these are almost identical to that for the X = Cl compound, shows that the failure to obtain good quality ^{199}Hg spectra for X = Br, I is not due to sample impurity, or to a more complicated solid-state structure for these compounds. The X = CN compound showed only single signals for the acetate carbon atoms, but the CN carbon signal was resolved into a doublet, this being the only evidence in the solid-state NMR spectra for the presence of two inequivalent molecules, as found in the crystal structure determination (see above). This signal showed further splitting into a 2:1 doublet, which is typical of the pattern expected for residual dipolar coupling to ^{14}N, which is not entirely removed by MAS because of the presence of ^{14}N ($I = 1$) quadrupole coupling [50,51]. It has been shown that the splitting s is proportional to χD, where χ is the ^{14}N quadrupole coupling constant and D is the dipolar coupling constant [51]. A similar splitting was also seen in the ^{13}C

Table 6
Solid-state ^{13}C NMR parameters for some mercury complexes (data for $Hg(OAc)_2$ from Ref. [20])

Complex	Carbon	$\delta(^{13}C)$/ppm	$\lvert^1J(^{199}Hg^{13}C)\rvert$/Hz	$\lvert^nJ(^{199}Hg^{13}C)\rvert$/Hz	$s(^{14}N)$/Hz
$Hg(OAc)_2$	CO	180.9		118 (^2J)	
		176.8		156 (^2J)	
	CH_3	24.7		176 (^3J)	
		24.3		195 (^3J)	
$Hg(CN)_2$	CN	148.5[a]	3315		232
Hg(CN)OAc	CO	182.2		—	
	CH_3	23.8		—	
	CN	135.9[a]			220
		134.3[a]			220
$Hg(SCN)_2$	SCN	129.4			
Hg(SCN)OAc	CO	180.6		119 (^2J)	
	CH_3	23.3		143 (^3J)	
	SCN	119.0			
Hg(Me)OAc	CH_3	−0.4	1850		
	CO(OAc)	177.4		—	
	CH_3(OAc)	24.9		—	
Hg(Cl)OAc	CO	181.2		—	
		179.2		—	
	CH_3	23.5		—	
Hg(Br)OAc	CO	180.7		—	
		178.6		—	
	CH_3	24.9		—	
Hg(I)OAc	CO	179.9		—	
		178.3		—	
	CH_3	27.1		—	

[a] Weighted average shift of a 2:1 doublet due to residual ^{14}N–^{13}C dipolar coupling (the more intense component of the doublet has the higher chemical shift); the doublet splitting s is given in the last column.

spectrum of $Hg(CN)_2$ (Table 6). This effect has also been observed previously in $K_2[Hg(CN)_4]$, where the splitting is about 350 Hz [50]. The differences in the observed splittings are presumably due mainly to differences in the ^{14}N quadrupole coupling constants, since the CN bond lengths in $Hg(CN)_2$ (1.14 Å) [52] and $K_2[Hg(CN)_4]$ (1.16 Å) [53] are similar to those in [Hg(CN)OAc] (1.14, 1.15 Å; Table 1).

Acknowledgements

We thank Dr. L.-J. Baker and Dr. J.M. Seakins for help with the syntheses and the vibrational spectroscopy. G.A.B. thanks the University of Auckland for the grant of a period of study leave. A.V.C. thanks The Royal Society and the University of Durham for financial support.

We are grateful to EPSRC for access to the National Solid-State NMR Service, based at Durham, to Dr. D.C. Apperley for running the NMR spectra, and to Professor J.A.K. Howard for access to X-ray diffraction facilities.

References

[1] U. Haeberlen, Adv. Magn. Reson. Suppl. 1 (1976).
[2] C.A. Fyfe, Solid State NMR for Chemists, C.F.C. Press, Guelph, 1983.
[3] R.K. Harris, Nuclear Magnetic Resonance Spectroscopy. Longman, Harlow, 1986.
[4] J.A. Davies, S. Dutremez, Coord. Chem. Rev. 114 (1992) 201.
[5] A. Sebald, NMR Basic Principles Prog. 31 (1994) 91.
[6] R.K. Harris, P. Jackson, L.H. Merwin, B.J. Say, J. Chem. Soc. Faraday Trans. 1 84 (1988) 3649.
[7] R.K. Harris, Chem. Brit. (1993) 601.
[8] M. Mehring, in: P. Diehl, E. Fluck, H. Günther, R. Kosfeld (Eds.), NMR. Basic Principles and Progress, vol. 11, Springer, Berlin, 1976.
[9] P. Diehl, E. Fluck, H. Günther, R. Kosfeld, J. Seelig (Eds.), NMR. Basic Principles and Progress, vols. 30–33, Springer, Berlin, 1994.
[10] E.O. Stejskal, J.D. Memory, High Resolution NMR in the Solid State, Oxford University Press, Oxford, 1994.
[11] J.G. Wright, M.J. Natan, F.M. MacDonnell, D.M. Ralston, T.V. O'Halloran, Prog. Inorg. Chem. 38 (1990) 323.
[12] R.K. Harris, A. Sebald, Magn. Reson. Chem. 25 (1987) 1058.
[13] F. Ambrosius, E. Klaus, T. Schaller, A. Sebald, Z. Naturforsch. Teil A: 50 (1995) 423.
[14] M.J. Natan, C.F. Millikan, J.G. Wright, T.V. O'Halloran, J. Am. Chem. Soc. 112 (1990) 3255.
[15] R.A. Santos, E.S. Gruff, S.A. Koch, G.S. Harbison, J. Am. Chem. Soc. 113 (1991) 469.
[16] M. Han, O.B. Peerson, J.W. Bryson, T.V. O'Halloran, S.O. Smith, Inorg. Chem. 34 (1995) 1187.
[17] G.A. Bowmaker, I.G. Dance, R.K. Harris, W. Henderson, I. Laban, M. Scudder, S.-W. Oh, J. Chem. Soc. Dalton Trans. (1996) 2381.
[18] C.J. Groombridge, Magn. Reson. Chem. 31 (1993) 380.
[19] K. Eichele, S. Kroeker, G. Wu, R.E. Wasylishen, Solid State NMR 4 (1995) 295.
[20] P.F. Barron, J. Organomet. Chem. 236 (1982) 157.
[21] R. Allmann, Z. Kristallogr. 138 (1973) 366.
[22] B. Kamenar, M. Penavic, Inorg. Chim. Acta 6 (1972) 191. B. Kamenar, M. Penavic, A. Hergold-Brundic, Croat. Chem. Acta 57 (1984) 145.
[23] T.D. Smith, Nature 209 (1966) 907.
[24] SAINT Version 4.050, Siemens Analytical X-ray Instruments Inc., Madison, WI, USA, 1995.
[25] G.M. Sheldrick, SHELXTL. Release 5. Siemens Analytical X-ray Instruments Inc., Madison, WI, USA, 1994.
[26] G.M. Sheldrick, Acta Crystallogr. Sect. A: 46 (1990) 467.
[27] G.M. Sheldrick, SHELXL-93. Program for the Refinement of Crystal Structures, University of Göttingen, Germany, 1993.
[28] T. Bjorholm, H.J. Jakobsen, J. Magn. Reson. 84 (1989) 204.
[29] (a) J.R. Ascenso, H. Bai, R.K. Harris, unpublished results. (b) R.K. Harris, L.H. Merwin, G. Hagele, J. Chem. Soc. Faraday Trans. 1 85 (1989) 1409.
[30] A.C. Olivieri, J. Magn. Reson. A 123 (1996) 207.
[31] J.M. Hook, P.A.W. Dean, L.C.M. van Gorkom, Magn. Reson. Chem. 33 (1995) 77.
[32] K. Brodersen, H.-U. Hummel, in: G. Wilkinson (Ed.), Comprehensive Coordination Chemistry, vol. 5, Pergamon, Oxford, 1987, p. 1047.
[33] W. Levason, C.A. McAuliffe, The coordination chemistry of mercury, in: C.A. McAuliffe (Ed.), The Chemistry of Mercury, McMillan, London, 1977.
[34] A.J. Canty, G.B. Deacon, Inorg. Chim. Acta 45 (1980) L225.
[35] A.F. Wells, Structural Inorganic Chemistry, Clarendon, Oxford, 5th edition, 1984, pp. 1156–1169.
[36] D. Grdenīc, Q. Rev. Chem. Soc. 19 (1965) 303.
[37] P.A.W. Dean, Prog. Inorg. Chem. 24 (1978) 109.
[38] S.C. Nyburg, C.H. Faerman, Acta Crystallogr. Sect. B: 41 (1985) 274.
[39] A. Bondi, J. Phys. Chem. 50 (1972) 977.
[40] G.A. Bowmaker, Adv. Spectrosc. 14 (1987) 1.
[41] L.H. Jones, J. Chem. Phys. 27 (1957) 665.
[42] J.D. Kennedy, W. McFarlane, J. Chem. Soc. Faraday Trans. 2 72 (1976) 1653.
[43] J. Jokisaari, P. Diehl, Org. Magn. Reson. 13 (1980) 359.
[44] R.E. Wasylishen, R.E. Lenkiski, C. Rodger, Can. J. Chem. 60 (1982) 2113.
[45] Y.K. Grishin, D.V. Bazhenov, Y.A. Ustynyuk, V.M. Mastikhin, Zh. Strukt. Khim. 28 (1987) 45; J. Struct. Chem. 28 (1987) 850.
[46] G.A. Bowmaker, A.V. Churakov, R.K. Harris, J.A.K. Howard, D.C. Apperley, submitted for publication.
[47] G.A. Webb, Factors contributing to the observed chemical shifts of heavy nuclei, in: P. Laszlo (Ed.), NMR of Newly Accessible Nuclei, vol. 1, Academic Press, New York, 1983, p. 79.
[48] C.J. Jameson, H.S. Gutowsky, J. Chem. Phys. 40 (1964) 1714.
[49] G.E. Hawkes, K.D. Sales, L.Y. Lian, R. Gobetto, Proc. R. Soc. London Ser. A: 424 (1989) 93. N.J. Clayden, C.M. Dobson, L.-Y. Lian, D.J. Smith, J. Magn. Reson. 69 (1986) 476.
[50] G. Wu, R. Wasylishen, J Phys. Chem. 97 (1993) 7863.
[51] N.A. Davies, R.K. Harris, A. Olivieri, Mol. Phys. 87 (1996) 669.
[52] R.C. Seccombe, C.H.L. Kennard, J. Organomet. Chem. 18 (1969) 243.
[53] P.N. Gerlach, B.M. Powell, J. Chem. Phys. 85 (1986) 6004.